Separation Science and Technology
Publication details, including instructions for authors and subscription information:
http://www.informaworld.com/smpp/title~content=t713708471

Groundwater Cleanup by *in-situ* Sparging. IV. Removal of Dense Nonaqueous Phase Liquid by Sparging Pipes

Susan D. Burchfield[a]; David J. Wilson[a]
[a] DEPARTMENT OF CHEMISTRY, VANDERBILT UNIVERSITY, NASHVILLE, TENNESSEE

To cite this Article Burchfield, Susan D. and Wilson, David J.(1993) 'Groundwater Cleanup by *in-situ* Sparging. IV. Removal of Dense Nonaqueous Phase Liquid by Sparging Pipes', Separation Science and Technology, 28: 17, 2529 — 2551
To link to this Article: DOI: 10.1080/01496399308017495
URL: http://dx.doi.org/10.1080/01496399308017495

SEPARATION SCIENCE AND TECHNOLOGY, **28**(17&18), pp. 2529–2551, 1993

Groundwater Cleanup by *in-situ* Sparging. IV. Removal of Dense Nonaqueous Phase Liquid by Sparging Pipes

SUSAN D. BURCHFIELD and DAVID J. WILSON
DEPARTMENT OF CHEMISTRY
VANDERBILT UNIVERSITY
NASHVILLE, TENNESSEE 37235

ABSTRACT

Mathematical models for describing the removal of dense nonaqueous phase liquid (DNAPL) droplets dispersed in a contaminated aquifer by air sparging are described. The sparging configurations considered are 1) a single air pipe discharging at the bottom of the aquifer and 2) a single horizontal slotted pipe discharging at the bottom of the aquifer. Diffusion transport of VOC is assumed to take place from spherical DNAPL droplets through a thick stagnant water layer in a porous medium to the moving aqueous phase. The dependence of removal rates on model parameters is explored.

INTRODUCTION

The removal of dense nonaqueous phase liquids (DNAPLs) from aquifers has turned out to be one of the most difficult of the problems facing the environmental engineer involved with remediation of contaminated sites. Most of these contaminants are chlorinated hydrocarbon solvents (trichloroethylene, perchloroethylene, 1,1,1-trichloroethane, etc.) which typically have fairly low water solubilities (roughly 1000 mg/L or less), and their diffusion constants in water, like all diffusion constants in condensed phases, are quite small. The kinetics of solution of these VOCs are therefore severely limited by the rate of diffusion, which results in extremely slow rates of cleanup by pump-and-treat methods.

Feenstra and Cherry (1) indicated the problems presented by DNAPLs in groundwater, and Schwille's (2) experiments showed most graphically

how these compounds rapidly sink down through an aquifer, leaving a residual trail of DNAPL ganglia held interstitially in the porous medium. Typically this residue amounts to 5–50 L/m^3. Powers, Louriero, Abriola, and Weber (3, 4) explored the kinetics of solution of "blobs" of DNAPL trapped in water-saturated media. They blamed low rates of mass transfer of VOC on 1) rate limited mass transport between the nonaqueous and aqueous phases (the solution process itself), 2) the tendency of mobile aqueous phase to bypass contaminated regions of low permeability, and 3) nonuniform flow resulting from aquifer heterogeneities.

A technique which may be helpful in accelerating the remediation of sites contaminated with DNAPL is air sparging. One modification of the technique (vacuum-vaporizer wells) was discussed by Herrling and Stamm (5), and Brown (6) described a somewhat simpler sparging technique which has been used in the United States for removing VOCs from groundwater. We have presented models for sparging dissolved VOCs by means of an aeration curtain extending at right angles to the direction of natural groundwater flow (7) and by means of a simple air injection well (8). A more recent model describes the removal of DNAPLs by means of vacuum-vaporizer type wells and by means of aeration curtains (9).

In the present paper we describe a model for removal of DNAPL by means of a sparging well consisting of a simple air injection pipe from which air is dispersed laterally as it rises through the aquifer. We also model the removal of DNAPL by means of a horizontal slotted pipe from which air is dispersed into the aquifer.

ANALYSIS

Sparging with a Single Air Injection Pipe

The configuration of the sparging system to be examined is shown in Fig. 1. Here air is injected at the bottom of the aquifer from a single pipe. It is assumed that the rate of natural groundwater movement is sufficiently slow that it can be neglected on the time scale of interest, so that the problem has axial symmetry. We shall use cylindrical coordinates r and z. Symbols are defined as follows.

h = thickness of aquifer, m
Q_a = molar air flow rate through the sparging well, mol/s
a_0 = maximum distance from the well at the top of the aquifer at which rising air is observed, m

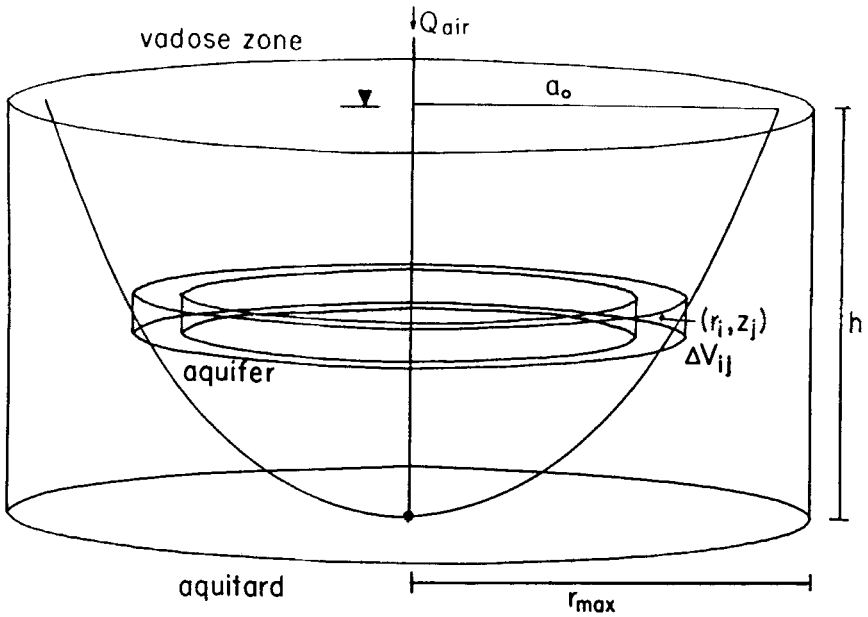

FIG. 1 Schematic diagram of a single vertical sparging well.

Let us assume a molar gas flux rate in the z-direction of

$$q_z(r, z) = A(a^2 - r^2), \text{ mol/m}^2\cdot\text{s}, \qquad r < a \tag{1}$$
$$= 0, \qquad r > a$$

Here we take

$$a = a(z) = a_0(z/h)^{1/2} \tag{2}$$

Then

$$Q_a = \int_0^a 2\pi A(a^2 - r^2) r dr \tag{3}$$
$$= \pi A a^4/2$$

which yields

$$A = \frac{2Q_a h^2}{\pi a_0^4 z^2} \tag{4}$$

So

$$q_z(r, z) = \frac{2Q_a}{\pi a_0^4} \frac{h^2}{z^2} [a_0^2(z/h) - r^2] \tag{5}$$

Now the molar gas flux in steady-state flow is conservative, so

$$\nabla q = 0 = \frac{1}{r} \frac{\partial}{\partial r} (rq_r) + \frac{\partial q_z}{\partial z} \tag{6}$$

This can be used with Eq. (5) to obtain the radial component of the molar gas flux, as follows. Differentiating $q_z(r, z)$ yields

$$\frac{\partial q_z}{\partial z} = \frac{2Q_a}{\pi a_0^4} \left[- \frac{2h^2}{z^3} [a_0^2(z/h) - r^2] + \frac{h^2}{z^2} \frac{a_0^2}{h} \right]$$

$$= \frac{2Q_a}{\pi a_0^4} \left[\frac{2r^2h^2}{z^3} - \frac{a_0^2 h}{z^3} \right] \tag{7}$$

From Eqs. (6) and (7) we have

$$\frac{1}{r} \frac{\partial}{\partial r} (rq_r) = - \frac{2Q_a}{\pi a_0^4} \left[\frac{2r^2h^2}{z^3} - \frac{a_0^2 h}{z^2} \right] \tag{8}$$

so

$$\frac{\partial}{\partial r} (rq_r) = - \frac{2Q_a}{\pi a_0^4} \left[\frac{2h^2r^3}{z^3} - \frac{a_0^2 hr}{z^2} \right] \tag{9}$$

Integrating from $r' = 0$ to $r' = r$ then gives

$$rq_r = - \frac{2Q_a}{\pi a_0^4} \left[\frac{h^2r^4}{2z^3} - \frac{a_0^2 hr^2}{2z^2} \right] \tag{10}$$

so

$$q_r = \frac{Q_a}{\pi a_0^4} \frac{h^2 r}{z^3} [a_0^2(z/h) - r^2] \tag{11}$$

Recall

$$q_z(r, z) = \frac{2Q_a}{\pi a_0^4} \frac{h^2}{z^2} [a_0^2(z/h) - r^2] \tag{5'}$$

Now what is needed for the model is the volumetric flux of gas rather than the molar flux. If we assume that the gas obeys the ideal gas law, the

components of the volumetric flux are given in terms of the components of the molar flux by

$$S_r = \frac{RT}{p} q_r \tag{12}$$

and

$$S_z = \frac{RT}{p} q_z \tag{13}$$

Let us take the total pressure as ambient plus hydrostatic to an adequate approximation, so

$$P(z) = P_a + \sigma(h - z) \tag{14}$$

where $\sigma = 1$ atm/10.336 m. Then

$$S_r = \frac{RT}{P_a + \sigma(h - z)} \frac{Q_a}{\pi a_0^4} \frac{h^2 r}{z^3} [a_0^2(z/h) - r^2] \tag{15}$$

and

$$S_z = \frac{RT}{P_a + \sigma(h - z)} \frac{2Q_a}{\pi a_0^4} \frac{h^2}{z^2} [a_0^2(z/h) - r^2] \tag{16}$$

with S_r and $S_z = 0$ if $r^2 > a_0^2(z/h)$.

We next turn to the mass balances for the volume elements. The volume of the ijth volume element is given by

$$V_{ij} = (2i - 1)\pi(\Delta r)^2 \Delta z \tag{17}$$

The areas of the top and bottom surfaces of the volume element are given by $(2i - 1)\pi(\Delta r)^2$. The area of the inner surface is $2(i - 1)\pi \Delta r \Delta z$, and the area of the outer surface is $2i\pi \Delta r \Delta z$.

Let

C_{ij} = DNAPL concentration in the ijth volume element, kg/m^3
c_{ij} = dissolved VOC concentration in the ijth volume element, kg/m^3 of aqueous phase
c_{ij}^g = gaseous VOC concentration in the ijth compartment, kg/m^3
ν = total porosity of medium
ω = water-filled porosity of medium
K_H = VOC Henry's constant, dimensionless
m_{ij} = total mass of VOC in ijth volume element

Then advective transport is described by

$$\frac{dm_{ij}}{dt} = S_{ij}^{B}(2i - 1)\pi(\Delta r)^2 c_{j-1}^{g} + S_{ij}^{I}2(i - 1)\pi\Delta r\Delta z c_{i-1,j}^{g} - S_{ij}^{T}(2i - 1)\pi(\Delta r)^2 c_{ij}^{g} - S_{ij}^{O}2i\pi\Delta r\Delta z c_{ij}^{g} \quad (18)$$

and

$$c_{ij}^{g} = K_H c_{ij} \quad (19)$$

on making the assumption that Henry's law applies. In Eq. (18), S_{ij}^{B} is the volumetric gas flux into the volume element through its bottom surface, S_{ij}^{I} is the flux in through the inner surface, S_{ij}^{T} is the flux through the top surface, and S_{ij}^{O} is the flux through the outer surface. These are defined as follows:

$$S_{ij}^{B} = S_z[(i - 1/2)\Delta r, (j - 1)\Delta z] \quad (20)$$

$$S_{ij}^{I} = S_r[(i - 1)\Delta r, (j - 1/2)\Delta z] \quad (21)$$

$$S_{ij}^{O} = S_r[i\Delta r, (j - 1/2)\Delta z] \quad (22)$$

$$S_{ij}^{T} = S_z[(i - 1/2)\Delta r, j\Delta z] \quad (23)$$

where S_r and S_z are defined in Eqs. (15) and (16), respectively. Calculating the total mass of VOC in the ijth volume element yields

$$m_{ij} = V_{ij}[C_{ij} + \omega c_{ij} + (\nu - \omega)c_{ij}^{g}] \quad (24)$$

For the kinetics of solution of the DNAPL droplets we take an expression derived for use in modeling the solution of DNAPL droplets by conventional pump-and-treat operations (10) in which it is assumed that the droplets are spherical in shape and that solution must take place through a stationary aqueous boundary layer of thickness large compared to the radius of the droplets. This gives

$$\frac{dC_{ij}}{dt} = -\frac{3C_0^{2/3}D(c_s - c_{ij})C_{ij}^{1/3}}{\rho\alpha_0^2} \quad (25)$$

where D = diffusivity of VOC in the water-saturated porous medium, m^2/sec
ρ = DNAPL density, kg/m^3
α_0 = initial DNAPL droplet radius, m
c_s = saturation concentration of VOC in water, kg/m^3

Now from the solution/diffusion process only we have

$$\left(\frac{\partial m_{ij}}{\partial t}\right)_{\text{diff}} = 0 = \Delta V_{ij}\left[\left(\frac{\partial C_{ij}}{\partial t}\right)_{\text{diff}} + [\omega - (\nu - \omega)K_{\text{H}}]\left(\frac{\partial c_{ij}}{\partial t}\right)_{\text{diff}}\right] \tag{26}$$

from which we obtain

$$\left(\frac{\partial c_{ij}}{\partial t}\right)_{\text{diff}} = -\frac{1}{[\omega + (\nu - \omega)K_{\text{H}}]}\frac{dC_{ij}}{dt} \tag{27}$$

Let the mass of VOC in the aqueous and vapor phases in ΔV_{ij} be μ_{ij}. Then

$$\mu_{ij} = \Delta V_{ij}[\omega + (\nu - \omega)K_{\text{H}}]c_{ij} \tag{28}$$

Now

$$\left(\frac{\partial \mu_{ij}}{\partial t}\right)_{\text{diff}} = -\Delta V_{ij}\frac{dC_{ij}}{dt} \tag{29}$$

and $(\partial\mu_{ij}/\partial t)_{\text{advect}}$ is given by the right side of Eq. (18). Then

$$\begin{aligned}\left(\frac{d\mu_{ij}}{dt}\right)_{\text{total}} = {} & -\Delta V_{ij}\frac{dC_{ij}}{dt} + S_{ij}^{\text{B}}(2i - 1)\pi(\Delta r)^2 c_{i,j-1}^{g} \\ & + S_{ij}^{\text{L}}2(i - 1)\pi\Delta r\Delta z c_{i-1,j}^{g} - S_{ij}^{\text{T}}(2i - 1)\pi(\Delta r)^2 c_{ij}^{g} \\ & - S_{ij}^{\text{O}}2i\pi\Delta r\Delta z c_{ij}^{g}\end{aligned} \tag{30}$$

Equation (28) yields

$$\frac{dc_{ij}}{dt} = \frac{1}{\Delta V_{ij}[\omega + (\nu - \omega)K_{\text{H}}]}\frac{d\mu_{ij}}{dt} \tag{31}$$

This, with Eq. (30), then yields

$$\begin{aligned}\frac{dc_{ij}}{dt} = {} & -\frac{1}{\omega + (\nu - \omega)K_{\text{H}}}\frac{dC_{ij}}{dt} + \frac{1}{\Delta V_{ij}[\omega + (\nu - \omega)K_{\text{H}}]} \\ & \times \{S_{ij}^{\text{B}}(2i - 1)\pi(\Delta r)^2 c_{i,j-1}^{g} + S_{ij}^{\text{L}}2(i - 1)\pi\Delta r\Delta z c_{i-1,j}^{g} \\ & - S_{ij}^{\text{O}}2i\pi\Delta r\Delta z c_{ij}^{g} - S_{ij}^{\text{T}}(2i - 1)\pi(\Delta r)^2 c_{ij}^{g}\}\end{aligned} \tag{32}$$

Now it is also necessary to take account of the fact that the gas is expanding as it rises, so that in the z-direction we must include a dilution factor for the c_{ij}^{g}. We assume that gas enters at the bottom of a volume element, rises (with expansion) to the middle, equilibrates with the liquid in this volume element at that point, and then rises (with expansion) out

through the top of the volume element. The dilution factors can readily be calculated; for gas rising from a height z_1 to a height z_2, we have

$$\frac{c^g(z_2)}{c^g(z_1)} = \frac{P_a + \sigma(h - z_2)}{P_a + \sigma(h - z_1)} \tag{33}$$

Including this dilution effect requires the following corrections. From the bottom of the i,jth volume element to the center of the i,jth volume element,

$$c^g[(i - 1/2)\Delta r, (j - 1/2)\Delta z] = c^g[(i - 1/2)\Delta r, (j - 1)\Delta z] \frac{P_a - \sigma[h - (j - 1/2)\Delta z]}{P_a + \sigma[h - (j - 1)\Delta z]} \tag{34}$$

From the middle of the $i,j - 1$th volume element to the bottom of the i,jth volume element,

$$c^g[(i - 1/2)\Delta r, (j - 1)\Delta z] = c^g[(i - 1/2)\Delta r, (j - 3/2)\Delta z] \frac{P_a + \sigma[h - (j - 1)\Delta z]}{P_a + \sigma[h - (j - 3/3)\Delta z]} \tag{35}$$

From the middle of the i,jth volume element to the top of the i,jth volume element,

$$c^g[(i - 1/2)\Delta r, j\Delta z] = c^g[(i - 1/2)\Delta r, (j - 1)\Delta z] \frac{P_a + \sigma[h - j\Delta z]}{P_a + \sigma[h - (j - 1/2)\Delta z]} \tag{36}$$

Let us define

$$P(k\Delta z) = P_a + \sigma(h - k\Delta z) \tag{37}$$

Then return to Eq. (32) and rescale the c_{ij}^g's to take this dilution by gas expansion into account. This yields

$$\begin{aligned}\frac{dc_{ij}}{dt} = & - \frac{1}{\omega + (\nu - \omega)K_H} \frac{dC_{ij}}{dt} + \frac{1}{\Delta V_{ij}[\omega + (\nu - \omega)K_H} \\ & \times \left[S_{ij}^B (2i - 1)\pi(\Delta r)^2 \frac{P[(j - 1)\Delta z]}{P[(j - 3/2)\Delta z]} c_{i,j-1}^g \right. \\ & + S_{ij}^L 2(i - 1)\pi \Delta r \Delta z c_{i-1,j}^g - S_{ij}^O 2i\pi \Delta r \Delta z c_{ij}^g \\ & \left. - S_{ij}^T (2i - 1)\pi(\Delta r)^2 \frac{P[j\Delta z]}{P[(j - 1/2)\Delta z]} c_{ij}^g \right]\end{aligned} \tag{38}$$

The model then consists of Eqs. (19), (25), and (38). The differential equations are integrated forward in time, Eq. (19) is used to calculate the gas phase VOC concentrations at each step, and the residual mass of contaminant in the domain of interest is calculated from the equation

$$M_{\text{total}} = \sum_{i,j} \Delta V_{ij}\{C_{ij} + [\omega + (\nu - \omega)K_H]c_{ij}\} \tag{39}$$

Sparging with a Single Horizontal Slotted Pipe

A diagram of the system is given in Fig. 2. Let

l = length of horizontal slotted pipe, m
h = thickness of aquifer, m
Q_a = molar air flow rate, mol/s

We assume a molar gas flux in the z-direction of

$$q_z(x, z) = A(a^2 - x^2), \qquad |x| < a \tag{40}$$
$$= 0, \qquad |x| > a$$

Then

$$Q_a = 2l \int_0^a A(a^2 - x^2)dx \tag{41}$$

$$= 4lAa^3/3 \tag{42}$$

So

$$A = 3fQ_a/4la^3 \tag{43}$$

We choose

$$a = a_0(z/h)^{1/2} \tag{44}$$

as before, so

$$A = \frac{3Q_a}{4la_0^3}(h/z)^{3/2} \tag{45}$$

So

$$q_z(x, z) = \frac{3Q_a}{4la_0^3}(h/z)^{3/2}[a_0^2(z/h) - x^2] \tag{46}$$

Now $\nabla q = 0$ for steady flow, which gives

$$\frac{\partial q_x}{\partial x} = -\frac{\partial q_z}{\partial z} \tag{47}$$

So

$$\frac{\partial q_x}{\partial x} = -\frac{\partial}{\partial z}\left[\frac{3Q_a}{4la_0^3}(h/z)^{3/2}[a_0^2(z/h) - x^2]\right] \tag{48}$$

$$= -\frac{3Q_a h^{3/2}}{4a_0^3 l}\left[-\frac{a_0^2}{2hz^{3/2}} + \frac{3x^2}{2z^{5/2}}\right] \tag{49}$$

Integrate Eq. (49) with respect to x' from 0 to x and note that $q_x(0, z) = 0$ to get

$$q_x(x, z) = \frac{3Q_a h^{3/2}}{8a_0^3 l}\frac{x}{z^{5/2}}[a_0^2(z/h) - x^2] \tag{50}$$

Recall

$$q_z(x, z) = \frac{3Q_a}{4la_0^3}(h/z)^{3/2}[a_0^2(z/h) - x^2] \tag{46'}$$

As before, the volumetric gas flux components are given by

$$S_x = (RT/P)g_x \tag{51}$$

and

$$S_z = (RT/P)q_z \tag{52}$$

Also, as before,

$$P(z) = P_a + \sigma(h - z) \tag{14'}$$

Then

$$S_x = \frac{RT}{P_a + \sigma(h - z)}\frac{3Q_a h^{3/2} x}{8a_0^3 l z^{5/2}}[a_0^2(z/h) - x^2] \tag{53}$$

and

$$S_z = \frac{RT}{P_a + \sigma(h - z)}\frac{3Q_a h^{3/2}}{4a_0^3 l z^{3/2}}[a_0^2(z/h) - x^2] \tag{54}$$

if $a_0^2(z/h) > x^2$. Also, $S_z = S_x = 0$ if $a_0^2(z/h) < x^2$.

We now turn to the calculation of the mass balances for the volume elements. Because of the symmetry of the problem, we need examine only the right half of the domain of interest. Let

$$x_i = (i - 1/2)\Delta x \tag{55}$$

$$y_j = (j - 1/2)\Delta y \tag{56}$$

The volume elements are of size

$$V = \Delta x \Delta z l \tag{57}$$

The inner and outer surfaces of a volume element are $l\Delta z$, and the upper and lower surfaces are $l\Delta x$. Other notation is as in the preceding section. See Fig. 2. Again we have

$$c_{ij}^g = K_H c_{ij} \tag{19'}$$

and

$$\frac{dC_{ij}}{dt} = -\frac{3C_0^2 D(c_s - c_{ij})C_{ij}^{1/3}}{\rho\alpha_0^2} \tag{25'}$$

Equation (32) is replaced by

$$\frac{dc_{ij}}{dt} = -\frac{1}{\omega + (\nu - \omega)K_H}\frac{dC_{ij}}{dt} + \frac{1}{\Delta V[\omega + (\nu - \omega)K_H]} \times \{S_{ij}^B l\Delta x c_{i,j-1}^g + S_{ij}^L l\Delta y c_{i-1,j}^g - S_{ij}^R l\Delta y c_{ij}^g - S_{ij}^T l\Delta x c_{ij}^g\} \tag{58}$$

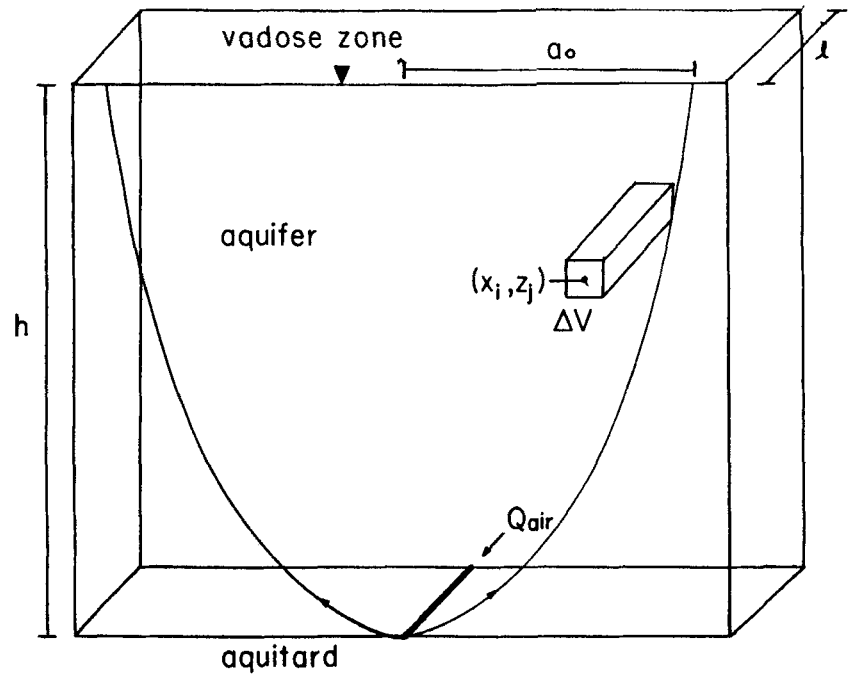

FIG. 2 Schematic diagram of a single horizontal slotted pipe sparging well.

Lastly, we need to correct the VOC concentrations at the top and bottom of the volume element for dilution effects as the rising gas expands. This is done in exactly the same way as was used to obtain Eq. (38); one obtains

$$\frac{dc_{ij}}{dt} = -\frac{1}{\omega + (\nu - \omega)K_H}\frac{dC_{ij}}{dt} + \frac{1}{\Delta V[\omega + (\nu - \omega)K_H}$$

$$\left[S_{ij}^{B} l \Delta x \frac{P[(j-1)\Delta z]}{P[(j-3/2)\Delta z]} c_{i,j-1}^{g} + S_{ij}^{L} l \Delta y c_{i-1,j}^{g} - \right.$$

$$\left. S_{ij}^{R} l \Delta y c_{ij}^{g} - S_{ij}^{T} l \Delta x \frac{P[j\Delta z]}{P[(j-1/2)\Delta z]} c_{ij}^{g}\right] \tag{59}$$

The gas fluxes are calculated from Eqs. (53) and (54) as follows.

$$S_{ij}^{B} = S_z[(i-1/2)\Delta x, (j-1)\Delta z] \tag{60}$$

$$S_{ij}^{L} = S_x[(i-1)\Delta x, (j-1/2)\Delta z] \tag{61}$$

$$S_{ij}^{R} = S_x[i\Delta x, (j-1/2)\Delta z] \tag{62}$$

$$S_{ij}^{T} = S_z[(i-1/2)\Delta x, j\Delta z] \tag{63}$$

To simulate a run, the model parameters are read in, the C_{ij} and c_{ij} are initialized, and Eqs. (25) and (58) are integrated forward in time. The c_{ij}^{g} are calculated from Eq. (19). The total residual mass of VOC is given by

$$M_{\text{total}} = \Delta V \sum_{i,j} \{C_{ij} + [\omega + (\nu - \omega)K_H]c_{ij}\} \tag{39}$$

RESULTS

Programs implementing these two sparging models were written in TurboBASIC and run on microcomputers using 80386 SX (16 MHz) and 80366 DX (33 MHz) microprocessors and math coprocessors. Typical runs required only a few minutes. Figures 3 through 9 pertain to sparging with a single vertical pipe; Figs. 10–12 to sparging with a buried horizontal slotted pipe. Default parameters for Figs. 3 through 9 are given in Table 1; default parameters for Figs. 10–12 in Table 2. The DNAPL characteristics were chosen to represent trichloroethylene unless otherwise specified.

Figure 3 shows plots of total mass of residual contaminant versus time for various sizes of the DNAPL droplets. Evidently the model is capable of representing quite severely diffusion-limited solutions of the DNAPL droplets if one selects droplet sizes which are relatively large. With the operating parameters used in these calculations, the sparging is definitely diffusion-limited, so we find that removal rates decrease like the reciprocal

TABLE 1
Default Parameters for Sparging with a Single Vertical Well

Thickness of aquifer	7 m
Radius of influence of air injection well at top of aquifer	7 m
N_z	7
N_r	7
Molar air flow rate of sparging well	1.96 mol/s
Ambient temperature	20°C
VOC Henry's constant (dimensionless)	0.35
VOC solubility in water	1100 mg/L
Soil density	1.7 g/cm^3
Total porosity of medium	0.4
Water-filled porosity of medium	0.36
Diffusion constant of VOC in porous medium	2×10^{-10} m^2/s
Density of VOC	1.46 g/cm^3
Initial DNAPL concentration	2000 mg/kg
Initial diameter of trapped DNAPL droplets	0.2 cm
Depth to which contaminant extends in aquifer	5 m
Radius to which contaminant extends about well	4 m
dt	900 seconds

of the square of the initial droplet radius, α_0. This is as one would expect from Eq. (25).

The effect of varying the Henry's constant of the DNAPL on the rate of DNAPL removal is shown in Fig. 4. Since the sparging is diffusion-limited, a marked decrease in Henry's constant (from 0.2 to 0.0025, dimensionless) results in only a slight decrease in removal rate. One expects that the effect of a decrease in Henry's constant would be larger if the gas flow rate through the sparging well were reduced to the point where the process is no longer so strongly diffusion-controlled; this was in fact found to be the case.

The effect of varying the aqueous solubility of the DNAPL (while holding Henry's constant unchanged) is shown in Fig. 5. Increases in solubility c_s result in very marked increases in removal rates, as one would expect from Eq. (25). In interpreting these results, one should note that as the solubility of the DNAPL is increased at constant K_H, the equilibrium vapor pressure of the DNAPL is increased proportionately. If, on the other hand, one holds the equilibrium vapor pressure constant while increasing the DNAPL solubility, K_H decreases proportional to $1/c_s$, which results in decreasing vapor-phase VOC concentrations according to Eq. (19). This tends to decrease removal rates. In the diffusion-limited regime the two effects virtually cancel each other out. At lower gas flow rates

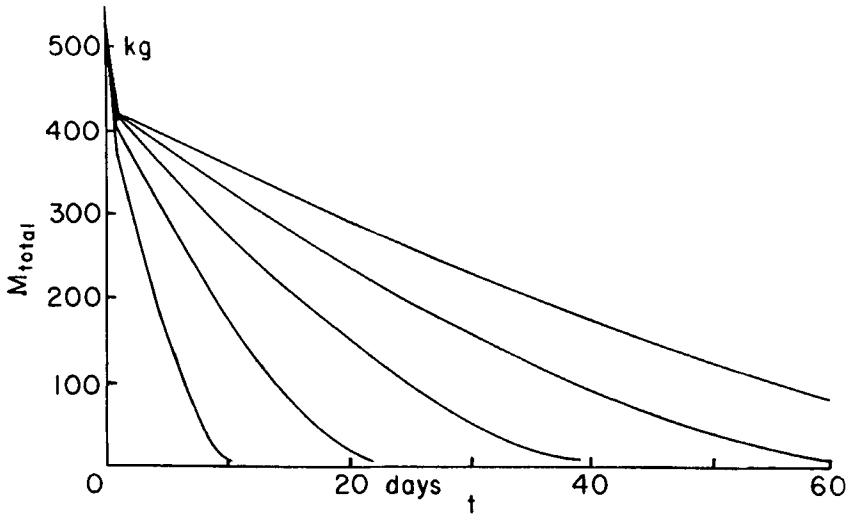

FIG. 3 Plots of residual contaminant mass versus time. Effect of DNAPL droplet size. From bottom to top, initial DNAPL droplet diameter = 0.10, 0.15, 0.20, 0.25, and 0.30 cm. Initial contaminant concentration = 1000 mg/kg. Other parameters as in Table 1.

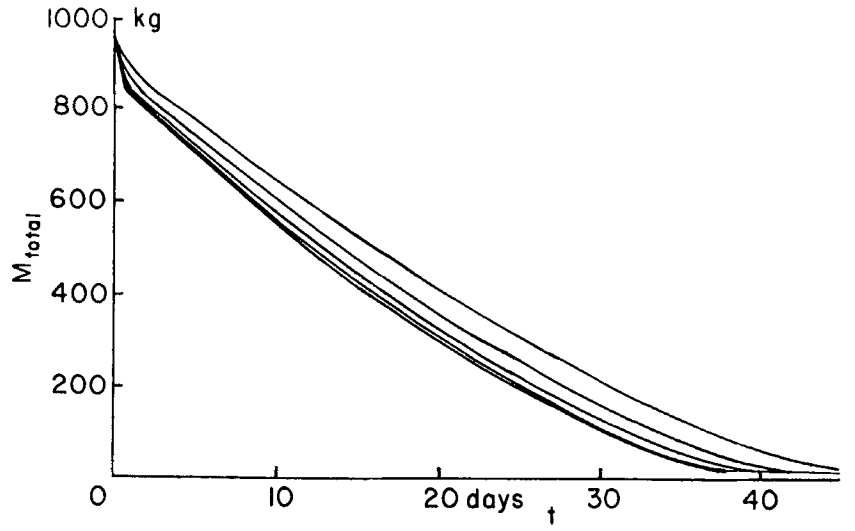

FIG. 4 Plots of residual contaminant mass versus time. Effect of VOC Henry's constant. From bottom to top, K_H = 0.2, 0.1, 0.05, 0.025, and 0.0125 (dimensionless). Other parameters as in Table 1.

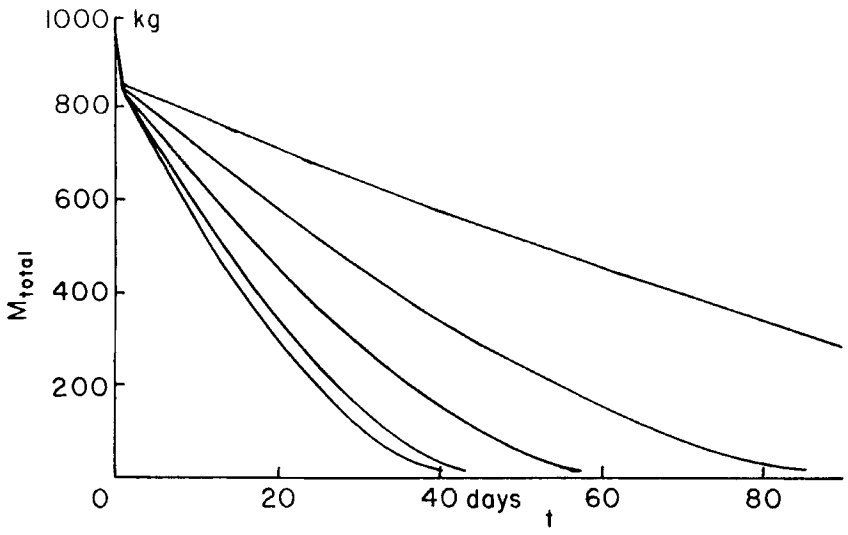

FIG. 5 Plots of residual contaminant mass versus time. Effect of DNAPL aqueous solubility. DNAPL solubility = 1100, 1000, 750, 500, and 250 mg/L, from bottom to top. Other parameters as in Table 1.

(where diffusion is no longer so limiting), removal rate decreases with increasing DNAPL solubility at constant DNAPL vapor pressure.

Figure 6 exhibits the effect of initial DNAPL concentration on removal rate. In these runs the DNAPL droplet size has been held constant, so the number of droplets per cubic meter is proportional to the DNAPL concentration. We therefore find, as expected, that the rate of DNAPL removal is directly proportional to the initial DNAPL concentration in the aquifer.

Decreases in the air flow rate of the sparging well result in decreases in the removal rate, as seen in Fig. 7. For the parameter sets used in these runs, diffusion kinetics are the dominant limiting factor in the removal. Therefore the results of decreasing the air flow rate are minor until one gets to flow rates of 0.1225 mol/s or so. It is apparent that excessively high flow rates result in little increase in removal rate if one is approaching the diffusion-limited regime. Such high air flow rates merely result in excessive energy costs for compressing air and also excessive treatment costs for removing VOCs from a high-volume, low-concentration exhaust gas stream if this must be done.

In this model the domain of the aquifer which is actually being aerated is assumed to be a paraboloid of revolution (see Eqs. 5 and 11). As long

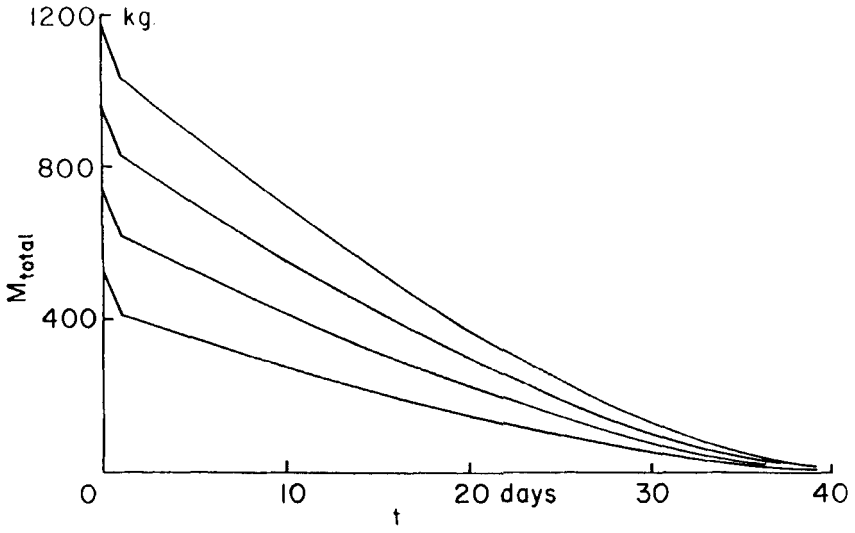

FIG. 6 Plots of residual contaminant mass versus time. Effect of initial DNAPL concentration in the aquifer. C_0 = 1000, 1500, 2000, and 2500 mg/kg, from bottom to top. Other parameters as in Table 1.

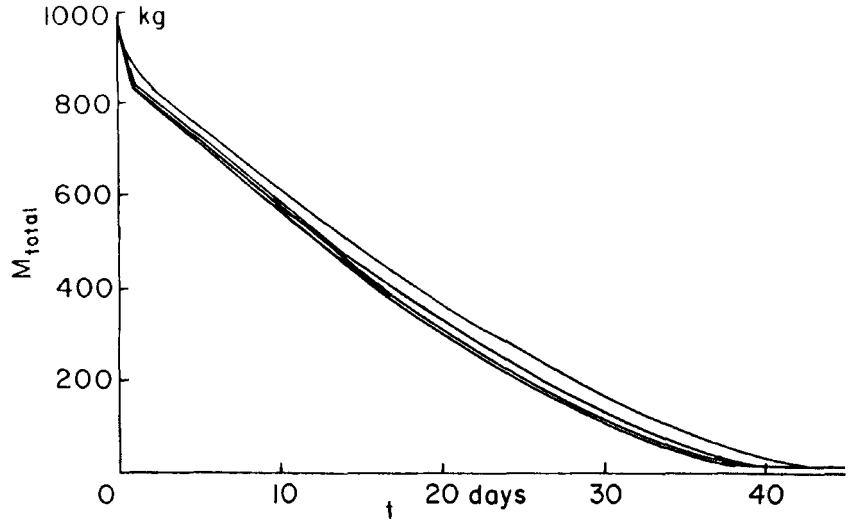

FIG. 7 Plots of residual contaminant mass versus time. Effect of sparging well air flow rate. Q = 0.98, 0.49, 0.245, and 0.1225 mol/s, from top to bottom. Other parameters as in Table 1.

as the zone of contamination lies entirely within this paraboloid of influence, one expects that complete remediation will occur. If, however, any of the contaminated region lies outside of this paraboloid, that domain will never be cleaned up. This is shown in Fig. 8, which shows plots of residual contaminant mass versus time for zones of contamination of several different radii. The two lowest curves correspond to zones of contamination lying wholly within the paraboloid of influence. The third has a quite small portion lying outside of the paraboloid, and the fourth has a rather substantial portion lying outside. For these last two plots we see that at large times the curves approach a positive limiting value for the residual contaminant mass. Since in these runs solution/diffusion of the DNAPL droplets is rate limiting, all the plots reach their final values of residual DNAPL at about the same time.

The effect of the depth to which the contamination extends is shown in Fig. 9. In four of the five runs the domain of contamination lies wholly within the paraboloid of influence of the well. In the fifth (top) run there is a small residual mass of DNAPL which is not removed, since the cylinder of contaminated aquifer extends beyond the paraboloid of influence of the sparging well near the bottom of the aquifer.

Figures 10–12 pertain to sparging with a buried horizontal slotted pipe. Model default parameters are given in Table 2. In Fig. 10 we see the effect

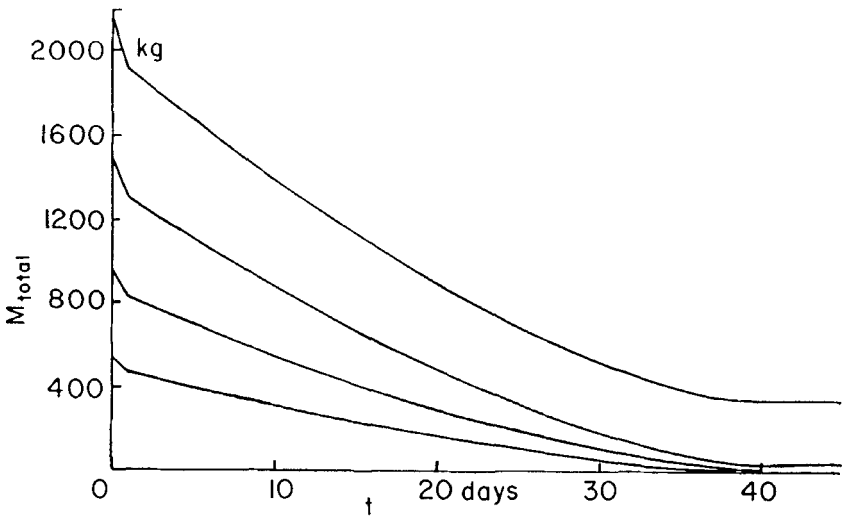

FIG. 8 Plots of residual contaminant mass versus time. Effect of radius of zone of contamination. Radius of zone of contamination = 3, 4, 5, and 6 m, from bottom to top. Other parameters as in Table 1.

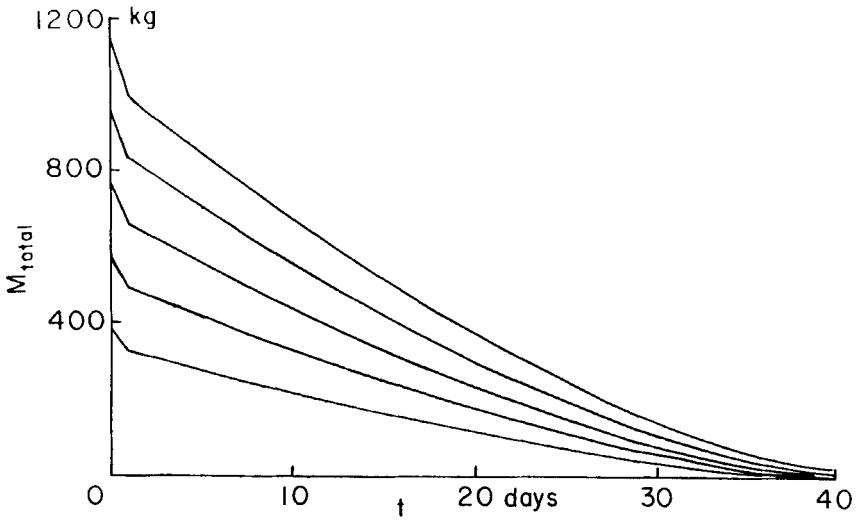

FIG. 9 Plots of residual contaminant mass versus time. Effect of depth of zone of contamination below the surface. The zone of contamination extends from the surface of the aquifer to depths of 2, 3, 4, 5, and 6 m, from bottom to top. Other parameters as in Table 1.

TABLE 2
Default Parameters for Sparging with a Single Buried Horizontal Slotted Pipe

Thickness of aquifer	7 m
Width of influence of air injection well at top of aquifer	14 m
N_z	7
N_x	7
Molar air flow rate of sparging well	1.96 mol/s
Ambient temperature	20°C
VOC Henry's constant (dimensionless)	0.35
VOC solubility in water	1100 mg/L
Soil density	1.7 g/cm^3
Total porosity of medium	0.4
Water-filled porosity of medium	0.36
Diffusion constant of VOC in porous medium	2×10^{-10} m^2/s
Density of VOC	1.46 g/cm^3
Initial concentration of DNAPL	2000 mg/kg
Initial diameter of trapped DNAPL droplets	0.2 cm
Depth to which contaminant extends in aquifer	5 m
Distance to which contaminant extends on either side of buried horizontal pipe	4 m
dt	900 seconds

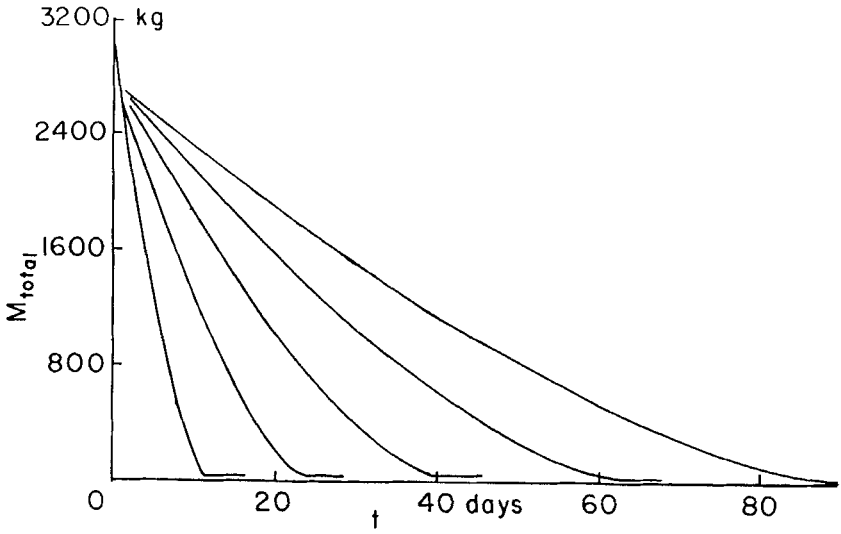

FIG. 10 Plots of residual contaminant mass versus time, horizontal pipe model. Effect of droplet size. Droplet diameters are 0.10, 0.15, 0.20, 0.25, and 0.30 cm, from bottom to top. Other parameters as in Table 2.

of increasing DNAPL droplet radius (i.e., progressively decreasing the diffusion/solution rate). The plots are very similar to those seen for the vertical pipe model which are given in Fig. 3. As before, removal rates are essentially proportional to α_0^2 since the systems are in the diffusion-limited regime.

The effect of variation in the sparging well air flow rate is seen in Fig. 11. At the lowest air flow rate (0.06125 mol/s, about 3 scfm) we see that the rate of advective removal is becoming the major bottleneck in the remediation. Evidently for this system air flow rates much larger than about 6 scfm will result in only modest increases in remediation rate.

Figure 12 exhibits the effect of the width of the zone of contamination (assumed to be a rectangular parallelepiped) on the course of the remediation. The zone of influence of the horizontal slotted pipe sparging well is assumed to be a parabolic cylinder (see Eqs. 46 and 50). As before, if the zone of contamination lies entirely within the domain of influence of the well, remediation is complete, as with the lower two plots. If, however, any of the zone of contamination lies outside of the domain of influence, contaminant in that portion of the zone will not be removed, as is seen for the upper two plots.

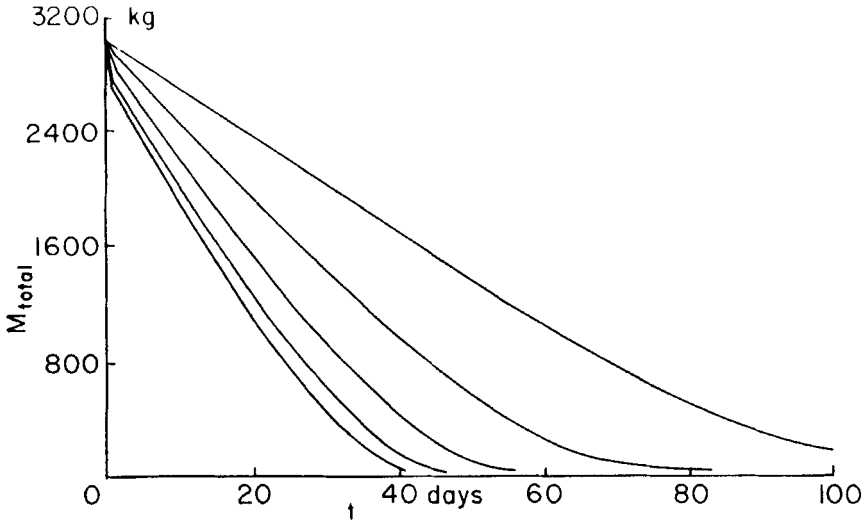

FIG. 11 Plots of residual contaminant mass versus time, horizontal pipe model. Effect of air flow rate. Q = 0.98, 0.49, 0.245, 0.1225, and 0.06125 mol/s, from bottom to top. Other parameters as in Table 2.

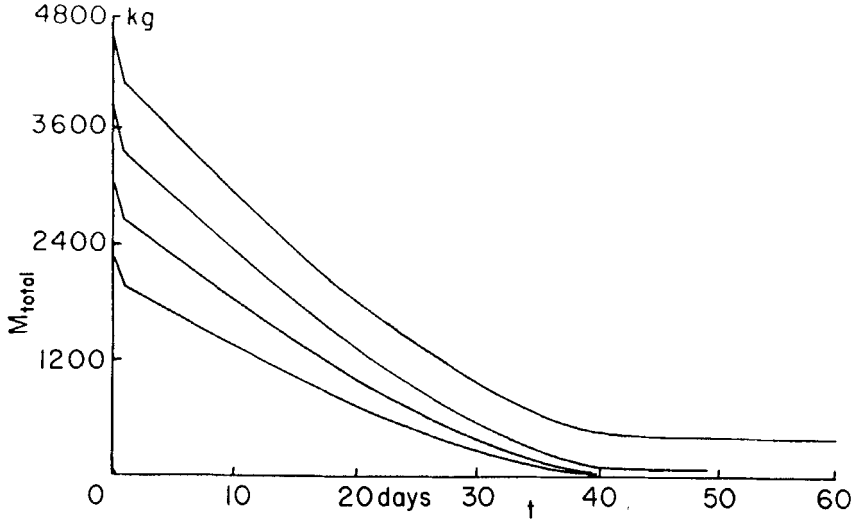

FIG. 12 Plots of residual contaminant mass versus time, horizontal pipe model. Effect of width of zone of contamination. Full width of zone of contamination = 6, 8, 10, and 12 m, from bottom to top. Other parameters as in Table 2.

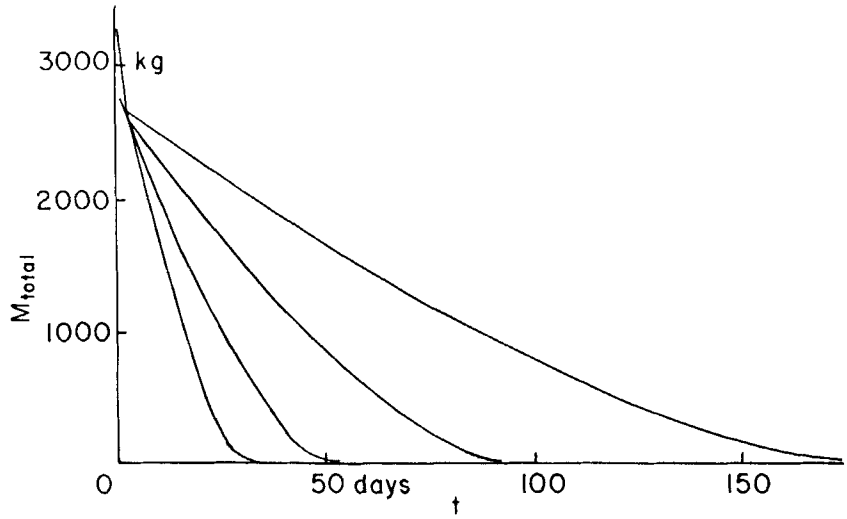

FIG. 13 Plots of residual contaminant mass versus time, horizontal slotted pipe model. Effect of varying DNAPL solubility at constant DNAPL vapor pressure, high sparging rate regime. Q_{air} = 0.98 mol/s. From left to right, (K_H, c_s) = (0.10, 2000 mg/L), (0.20, 1000 mg/L), (0.40, 500 mg/L), and (0.80, 250 mg/L). Other parameters as in Table 2.

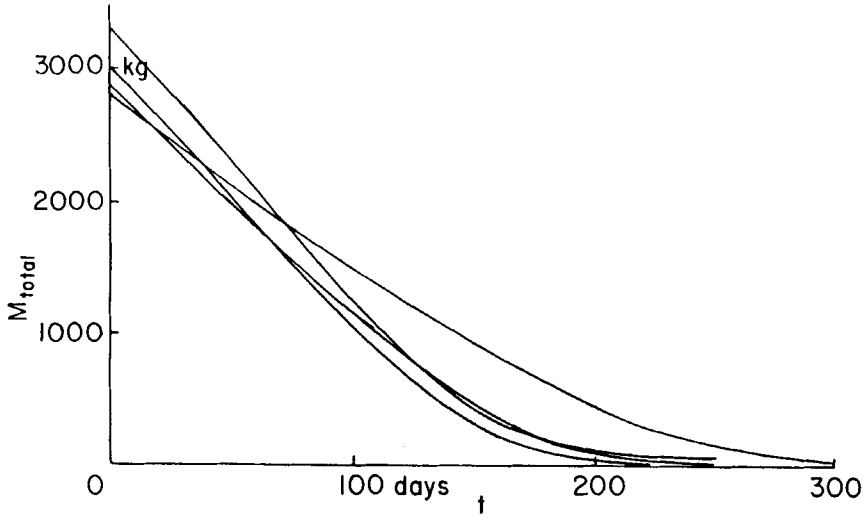

FIG. 14 Plots of residual contaminant mass versus time, horizontal slotted pipe model. Effect of varying DNAPL solubility at constant DNAPL vapor pressure, low sparging rate regime. Q_{air} = 0.06125 mol/s. From left to right, (K_H, c_s) = (0.10, 200 mg/L), (0.20, 1000 mg/L), (0.40, 500 mg/L), and (0.80, 250 mg/L). Other parameters as in Table 2.

The effects of varying the DNAPL solubility while holding its vapor pressure constant are shown in Figs. 13 and 14. In Fig. 13 the sparging gas flow rate is rather large (0.98 mol/s), and we find for this situation (where diffusion is definitely rate limiting) that the rate of removal is essentially proportional to the aqueous solubility of the DNAPL. The situation is rather different if the sparging gas flow rate is only 0.0615 mol/s, as is the case in Fig. 14. We find that removal rates decrease with decreasing solubility, but the effect is very much smaller. Recall that in Figs. 13 and 14 the vapor pressure of the DNAPL is being held constant, so that at low sparging gas flow rates the concentration of VOC in the advecting gas is determined essentially by the equilibrium vapor pressure of the DNAPL rather than by the rate of diffusion from the DNAPL droplets. The observed differences between Figs. 13 and 14 are therefore exactly as one would expect.

CONCLUSIONS

The models presented here enable one to get some insight into the factors affecting the sparging of DNAPL droplets/ganglia/blobs from contaminated aquifers. The model for solution/diffusion permits one to represent a virtually infinite range of rates for this process. The number of parameters required to use the models is relatively modest, and most of these are readily obtained. Computationally, the models are sufficiently simple that they can be run on readily available microcomputers.

On the other hand, the models also focus attention on aspects of sparging which require further study. Some of these are as follows.

1. We have postulated the form of the flow field of the sparge gas, which is an approach leaving something to be desired in terms of rigor, even if the postulated flow field seems "reasonable." Solution of this problem in terms that permit microcomputer modeling may be rather difficult. In particular, we have little insight into the relationship between air flow rate, thickness of aquifer, and the radius of the circle at the top of the aquifer through which air is moving, a_0. Intuitively one expects that a_0 increases with increasing air flow rate Q, but we do not know the functional dependence.

2. We have assumed local equilibrium between the dissolved VOC and the VOC in the vapor phase. This approximation could be replaced without much difficulty by some kind of lumped parameter approach as experimental results become available indicating that the kinetics of VOC mass transfer between the liquid and vapor phases is a significant factor.

3. We have assumed that the flow field of the sparging air induces no bulk movement of the water in the aquifer. Some preliminary bench-scale experiments were carried out in which dye is put into the pool of liquid at the top of a sand bed in which air sparging is taking place, and the attenuation of the dye is then followed with time as sparging continues. These indicated that the rate of mixing of the liquid in the sand bed with the overlying liquid is quite slow, suggesting that this assumption may be reasonable. One would expect, however, that a rigorous theoretical treatment will be difficult and probably beyond the scope of computer models suitable for use on microcomputers.

REFERENCES

1. S. Feenstra and J. A. Cherry, "Dense Organic Solvents in Ground Water: An Introduction," in *Dense Chlorinated Solvents in Ground Water* (Progress Report 0863985), Institute for Ground Water Research, University of Waterloo, Waterloo, Ontario, Canada, 1987.
2. F. Schwille, *Dense Chlorinated Solvents in Porous and Fractured Media: Model Experiments* (J. F. Pankow, trans.), Lewis Publishers, Chelsea, Michigan, 1988.
3. S. E. Powers, C. O. Louriero, L. M. Abriola, and W. J. Weber Jr., "Theoretical Study of the Significance of Nonequilibrium Dissolution of Nonaqueous Phase Liquids in Subsurface Systems," *Water Resour. Res.*, *27*, 463–477 (1991).
4. S. E. Powers, L. M. Abriola, and W. J. Weber Jr., "An Experimental Investigation of Nonaqueous Phase Liquid Dissolution in Saturated Subsurface Systems," *Ibid.*, *28*, 2691–2705 (1992).
5. B. Herrling and J. Stamm, *Vacuum-Vaporizer-Wells for In Situ Remediation of Volatile and Strippable Contaminants in the Unsaturated and Saturated Zone*, Presented at the Symposium on Soil Venting, Houston, Texas, April 29–May 1, 1991, Robert S. Kerr Environmental Research Laboratory and National Center for Ground Water Research, sponsors.
6. R. A. Brown, *Air Sparging—Extending Volatilization to Contaminated Aquifers*, Presented at the Symposium on Soil Venting, Houston, Texas, April 29–May 1, 1991, Robert S. Kerr Environmental Research Laboratory and National Center for Ground Water Research, sponsors.
7. D. J. Wilson, S. Kayano, R. D. Mutch Jr., and A. N. Clarke, "Groundwater Cleanup by *in-situ* Sparging. I. Mathematical Modeling," *Sep. Sci. Technol.*, *27*, 1023–1041 (1992).
8. D. J. Wilson, "Groundwater Cleanup by *in-situ* Sparging. II. Modeling of Dissolved Volatile Organic Compound Removal," *Ibid.*, *27*, 1675–1690 (1992).
9. L. A. Roberts and D. J. Wilson, "Groundwater Cleanup by *in-situ* Sparging. III. Modeling of Dense Nonaqueous Phase Liquid Droplet Removal," *Ibid.*, *28*, 1127–1143 (1993).
10. S. Kayano and D. J. Wilson, "Migration of Pollutants in Groundwater. VI. Flushing of DNAPL Droplets/Ganglia," *Environ. Monitor. Assess.*, *25*, 193–212 (1993).

Received by editor April 12, 1993